

Manipulation of tunnelling in a quantum dot array

This article has been downloaded from IOPscience. Please scroll down to see the full text article.

2005 J. Phys.: Condens. Matter 17 4207

(<http://iopscience.iop.org/0953-8984/17/26/018>)

View [the table of contents for this issue](#), or go to the [journal homepage](#) for more

Download details:

IP Address: 129.252.86.83

The article was downloaded on 28/05/2010 at 05:13

Please note that [terms and conditions apply](#).

Manipulation of tunnelling in a quantum dot array

Zhe Jiang¹, Duan Suqing and XianGeng Zhao

Institute of Applied Physics and Computational Mathematics, PO Box 8009, Beijing 100088, People's Republic of China

E-mail: jzher@yahoo.com

Received 19 April 2005, in final form 5 June 2005

Published 17 June 2005

Online at stacks.iop.org/JPhysCM/17/4207

Abstract

In this paper we present a method to control the electronic position in a quantum dot array coherently with a two-electron model. In this novel phenomenon, we find that the external ac driving field has a good manipulative effect on the tunnelling, and therefore the penetrability of the barrier can be easily adjusted. Through studying the Floquet spectrum of the system, we find that it can be divided into two minibands. The upper miniband describes the physical process of states in which the two electrons stay in the same dot and the lower miniband describes the states in which the two electrons stay in different dots. The parameter regions in which the manipulation of tunnelling is investigated exactly correspond to the collapse zones of quasi-energy levels.

(Some figures in this article are in colour only in the electronic version)

1. Introduction

The manipulation and control of a quantum state has been a long-term goal with important applications in quantum computation [1–3]. Recent progress in fabrication technology facilitates study in this area, and great advances have been achieved. One of the useful tools to control the quantum state is the ac electric field, which can coherently manipulate the time development of electronic states in a quantum dot (QD) system. A good example of the effect of ac field is the phenomenon of ‘dynamical localization’, which was first discovered by Grossmann [4, 5]. Through the coherent destruction of tunnelling (CDT), the electrons can be completely localized in their initial state [6, 7], which provides an effective method to dynamically control the quantum states. For that reason, this phenomenon has attracted a lot of interest and much work has been done. The double QD molecule, since it is intrinsic and essential, has been studied by many people [8–10]. The localization effect of some other kinds of quantum devices, such as the square QD molecule [11, 12] and QD array [13, 14], has also been intensively researched. In recent works, Zhang studied the frequency-dependent

¹ Author to whom any correspondence should be addressed.

electrical transport under intense terahertz radiation [15, 16]; Platero studied the photon-assisted transport in semiconductor nanostructures [17]; Kohler [18] researched the prospects to control by use of time-dependent fields quantum transport phenomena in nanoscale systems; these are all interesting applications of the CDT. In studies of the CDT, people have found that the system shows localization of the two interacting electrons in both cases of it starting from either a localized or a delocalized state. These novel phenomena can be successfully analysed by the Floquet approach, which believes that the localization occurs when two quasi-energies of states participating in the dynamics approach each other, and become either degenerate or close to degenerate. This phenomenon of quasi-energy collapse happens not only in the QD system but also in the superlattice. In this latter case the quasi-energy minibands collapse at some special values of field magnitude [19, 20].

Although dynamical localization is an important approach to manipulate the quantum states, localizing the electrons only in their initial states cannot satisfy the demand of quantum computation. In a recent paper [21], Villas-Boas presents an interesting method to selectively suppress the tunnelling between QDs through simply tuning the ac field intensity between two kinds of values with a one-electron model. In this paper, with the help of the long-time averaged occupation probability (LAOP) method [22], we study the manipulation of tunnelling in a two-electron model. The system studied here is a QD array under the action of an external ac field, of which the Floquet spectrum can be divided into two minibands. With appropriate ac field intensity, these two electrons can maintain their initial state forever. If the initial state is a double occupation state, which means that the two electrons both occupy the same dot, the parameters with which localization happens exactly correspond to the crossing points of the upper miniband. On the other hand, if the initial state is a single occupation state, which means that the two electrons occupy different dots, the parameters precisely correspond to the crossing points of the lower miniband. When the field intensity deviates from the localization values, the localization is destroyed and the electrons begin to oscillate. Through adjusting the field intensity, we can easily change the penetrability of the barriers, and therefore the position of the electrons in the array can be controlled.

This paper is organized as follows. The second section describes the LAOP method as applied in this paper. Section 3 contains a discussion about the manipulation of tunnelling with an initial double occupation state. Section 4 presents the discussion concerning the manipulation of tunnelling with an initial single occupation state. With the help of the Floquet approach, we further explain the physical process of the manipulative effect in section 5. A summary and conclusion are given in section 6.

2. LAOP method

We consider a quantum system under the action of periodic field. Since the Hamiltonian $H(t)$ has the property of time periodicity, we can describe the quantum evolution of the system in terms of the Floquet formalism. The quasi-energy wavefunction of the Hamiltonian H can be written as $|\phi_\alpha(t)\rangle = \exp(-i\varepsilon_\alpha t)|u_\alpha(t)\rangle$ with $|u_\alpha(t)\rangle = |u_\alpha(t+T)\rangle$, where ε_α is the quasi-energy, T is the period of the external field, and $|u_\alpha(t)\rangle$ satisfies the eigenvector equation (henceforth $\hbar = 1$)

$$\left(H(t) - i\frac{\partial}{\partial t}\right)|u_\alpha(t)\rangle = \varepsilon_\alpha|u_\alpha(t)\rangle. \quad (1)$$

We can integrate numerically the equation

$$i\frac{\partial}{\partial t}U(t, 0) = H(t)U(t, 0), \quad (2)$$

and diagonalize $U(T, 0) = S \exp(-iD)S^\dagger$ to obtain the quasi-energy ε and the initial Floquet state $|u(0)\rangle$ [23]. We suppose $|\varphi_m\rangle$ is a set of real-space basis vectors of this system which has M dimensions and give an initial state of the system $|\psi(0)\rangle$ which is a member of the vectors $|\varphi_m\rangle (m = 1, \dots, M)$. Then the time evolution of the system can be expressed in terms of Floquet states as follows:

$$|\psi(t)\rangle = \sum_{\alpha=1}^M \exp(-i\varepsilon_\alpha t) |u_\alpha(t)\rangle \langle u_\alpha(0) | \psi(0)\rangle. \quad (3)$$

Using the above equation, we can easily get

$$U(t, 0) = \sum_{\alpha=1}^M \exp(-i\varepsilon_\alpha t) |u_\alpha(t)\rangle \langle u_\alpha(0) |, \quad (4)$$

and we can get $|u_\alpha(t)\rangle$ at arbitrary time $t \in [0, T]$ by using equation (4) through the midway results of calculating $U(T, 0)$.

We describe the Floquet state as

$$|u_\alpha(t)\rangle = \sum_{m=1}^M c_{\alpha,m}(t) |\varphi_m\rangle. \quad (5)$$

Supposing $|\psi(0)\rangle = |\varphi_\gamma\rangle$, we can get

$$|\psi(t)\rangle = \sum_{\alpha=1}^M \sum_{m=1}^M c_{\alpha,\gamma}^*(0) c_{\alpha,m}(t) \exp(-i\varepsilon_\alpha t) |\varphi_m\rangle, \quad (6)$$

through equations (3) and (5).

To investigate the dynamical effect of the system, we define $P(t)$ as the occupation probability of the component of state $|\varphi_\zeta\rangle$ in the state $|\psi(t)\rangle$. Using equation (6), we can get

$$P(t) = \sum_{\alpha=1}^M |c_{\alpha,\gamma}(0)|^2 |c_{\alpha,\zeta}(t)|^2 + 2 \operatorname{Re} \sum_{\alpha=1}^{M-1} \sum_{\beta=\alpha+1}^M c_{\alpha,\gamma}(0) c_{\beta,\gamma}^*(0) c_{\alpha,\zeta}^*(t) c_{\beta,\zeta}(t) \exp[-i(\varepsilon_\beta - \varepsilon_\alpha)t]. \quad (7)$$

Defining $P_{|\varphi_\gamma\rangle, |\varphi_\zeta\rangle}$ to express the long-time averaged value of $P(t)$, with initial state $|\varphi_\gamma\rangle$ and final state $|\varphi_\zeta\rangle$, we can get [22]

$$\begin{aligned} P_{|\varphi_\gamma\rangle, |\varphi_\zeta\rangle} &= \lim_{\tau \rightarrow \infty} \frac{1}{\tau} \int_0^\tau P(t) dt = \lim_{N \rightarrow \infty} \frac{1}{NT} \sum_{n=1}^N \int_0^T P(t + (n-1)T) dt \\ &= \lim_{Q \rightarrow \infty} \frac{1}{Q} \sum_{q=0}^{Q-1} \sum_{\alpha=1}^M |c_{\alpha,\gamma}(0)|^2 \left| c_{\alpha,\zeta} \left(\frac{qT}{Q} \right) \right|^2 \\ &\quad + 2 \operatorname{Re} \lim_{Q \rightarrow \infty} \frac{1}{Q} \sum_{q=0}^{Q-1} \sum_{\alpha=1}^{M-1} \sum_{\beta=\alpha+1}^M \delta(\varepsilon_\beta - \varepsilon_\alpha) c_{\alpha,\gamma}(0) c_{\beta,\gamma}^*(0) c_{\alpha,\zeta}^* \left(\frac{qT}{Q} \right) c_{\beta,\zeta} \left(\frac{qT}{Q} \right). \end{aligned} \quad (8)$$

From equation (8), we can get the long-time averaged occupation probability (LAOP) $P_{|\varphi_\gamma\rangle, |\varphi_\zeta\rangle}$ through diagonalizing $U(T, 0)$. The value of $P_{|\varphi_\gamma\rangle, |\varphi_\zeta\rangle}$ can be used to describe the time evolution quantitatively. If $|\varphi_\zeta\rangle = |\varphi_\gamma\rangle$, and if $P_{|\varphi_\gamma\rangle, |\varphi_\zeta\rangle} \approx 1$, the electrons will contain their initial state $|\varphi_\gamma\rangle$ forever. Similarly, if $|\varphi_\zeta\rangle \neq |\varphi_\gamma\rangle$ and $P_{|\varphi_\gamma\rangle, |\varphi_\zeta\rangle} \approx 1$, we

know the electrons transfer completely from state $|\varphi_\gamma\rangle$ to state $|\varphi_\zeta\rangle$. Further, supposing $P_{3s} = P_{|1\rangle,|1\rangle} + P_{|1\rangle,|2\rangle} + P_{|1\rangle,|3\rangle}$, (the subscript '3' and 's' means that it is the sum of the three final states), and supposing $P_{3s} \approx 1$, we know the electrons whose initial state is $|1\rangle$ are completely trapped in these three states of $|1\rangle$, $|2\rangle$ and $|3\rangle$. In practical calculations, the value of Q is finite and we can adjust this value to satisfy the precision we need. Since we can use the midway results of calculating $U(T, 0)$, the cost of calculation to obtain $P_{|\varphi_\gamma\rangle,|\varphi_\zeta\rangle}$ is only a little larger than that of the quasi-energy, which means that the value of $P_{|\varphi_\gamma\rangle,|\varphi_\zeta\rangle}$ can be obtained as conveniently as the quasi-energy.

As we pointed out in the introduction, the Floquet spectrum method is very useful in the study of the CDT. However, this method still has a shortcoming that the crossing or avoided crossing is only necessary but not sufficient evidence for localization. In simple systems, for example, the one-electron model or two-electron double QDs, the effect of this shortcoming is small. But if we consider a more complicated system, like the model studied in this paper, it is very difficult to get useful information directly through the Floquet spectrum because the Floquet spectrum is too complex and there are too many crossing (avoided crossing) points. A good example is [13]. In that paper, the quasi-energy levels are carefully selected before being used and even though, since the crossing is not sufficient evidence, we do not know whether the localization happens directly from the treated Floquet spectrum. To solve this problem, Creffield further calculated the minimum value of occupation probability during ten periods of the driving field and found some CDT properties. The cost of computation to solve this minimum value is much larger than that to solve the Floquet spectrum. Unfortunately, after so much computation, we still cannot know the dynamics of system even at the 11th driving period. Thus, the efficiency of those above methods is not satisfying.

Now, all of these above problems can be easily solved through the LAOP method. As we mentioned above, after evolving the system only for one driving period (from $t = 0$ to T), we can get the LAOP, which determines that the computation cost of the LAOP method is similar to that of the Floquet spectrum. But through this simple process we can directly get the averaged value of the occupation probability from $t = 0$ to $+\infty$. Moreover, it is clear that the LAOP is the necessary and sufficient condition of dynamical localization. Since the LAOP method has those advantages, it is the prime method used in this paper.

3. Manipulation of tunnelling with initial double occupation state

We consider a QD array which contains seven coupling quantum dots. Since there are two electrons in this QD array, with a Hubbard model of a single-band system in an ac electric field $E(t)$, the model Hamiltonian of this system can be written as [13, 14]

$$H = W \sum_{\sigma,m} (a_{m,\sigma}^\dagger a_{m+1,\sigma} + a_{m+1,\sigma}^\dagger a_{m,\sigma}) - e d E(t) \sum_{\sigma,m} m a_{m,\sigma}^\dagger a_{m,\sigma} + U \sum_m N_{m,\uparrow} N_{m,\downarrow}, \quad (9)$$

where $a_{m,\sigma}^\dagger$ ($a_{m,\sigma}$) creates (annihilates) an electron with spin σ on the m th site, W describes the coupling between the nearest-neighbour dots, d is the lattice constant, and U is the Coulomb interaction in one dot. The external field is

$$E(t) = E \cos \omega t, \quad (10)$$

where E and ω are the amplitude and frequency of the ac field.

Since there are two electrons in the system, we can write the Hamiltonian equation (9) in the space spanned by the two-particle basis vectors as [8–10]

$$H(t) = \begin{bmatrix} H_3 & 0 \\ 0 & H_1 \end{bmatrix}, \quad (11)$$

where H_3 corresponds to the triplet subspace and H_1 describes the singlet subspace. For the reason that equation (9) contains no spin-flip terms, there is no mixture of singlet and triplet subspace. Therefore if the spin of the initial state locates in the singlet subspace, the system will preserve this property in the process of evolution and we can focus our attention only on this subspace. In the singlet subspace, we use $|k, l\rangle$ to describe the two-particle basis vectors, which means one electron in the k th dot and the other one in the l th. Then the reduced Hamiltonian H_1 can be written as

$$\begin{aligned} \langle m, n | H_1 | k, l \rangle = & 2^{\frac{\delta_{k,l}}{2}} W (\delta_{m,k-1} \delta_{n,l} + \delta_{m,k} \delta_{n,l+1}) - (k+l) e d E(t) \delta_{m,k} \delta_{n,l} \\ & + 2^{\frac{\delta_{k+1,l}}{2}} (2 - 2^{\delta_{k,l}}) W (\delta_{m,k+1} \delta_{n,l} + \delta_{m,k} \delta_{n,l-1}) + \delta_{k,l} U \delta_{m,k} \delta_{n,l}. \end{aligned} \quad (12)$$

In this paper, we set ω as the unit and define $\mu = edE/\omega$. In the studied range of the parameters, it can be found that the LAOP with $Q = 10, 20$ and 50 will be almost same. Thus, we know $Q = 10$ is adequate and set $Q = 10$ for all calculations displayed in this paper. The coupling studied in this paper is $W/\omega = 0.25$, and we suppose that the Coulomb interaction is $U/\omega = 2.3$.

The initial state used in this part is $|4, 4\rangle$, which means the two electrons are both in the fourth dot. Then we present the LAOP as a function of the electric field parameter μ , as shown in figure 1. In figure 1(a), the black solid line represents the LAOP of $P_{|4,4\rangle,|4,4\rangle}$, which means that the initial state and the final state are both $|4, 4\rangle$. The red dotted line denotes the LAOP of P_{3s} , where $P_{3s} = \sum_{j \geq i=3}^5 P_{|4,4\rangle,|i,j\rangle}$, which means the LAOP of two electrons trapped in the middle three dots. The blue dashed line describes the LAOP of P_{5s} , where $P_{5s} = \sum_{j \geq i=2}^6 P_{|4,4\rangle,|i,j\rangle}$, which means the LAOP of two electrons restricted in the middle five dots. One can see that there are peaks for all of these three curves and the positions of these peaks for these curves are nearly identical. In order to judge what takes place in the region near these peaks, we present an enlargement of figure 1(a), as shown in figure 1(b). In this figure, we can see that there are apparent differences between these three curves. In the middle of this figure, there are two sharp black solid peaks ($P_{|4,4\rangle,|4,4\rangle}$). If we select the ac field intensity as same as those two peaks, for example, $\mu = 14.8553$, based on the above discussion, those electrons can be localized in the fourth dot forever. The curve of P_{3s} is obviously separated from $P_{|4,4\rangle,|4,4\rangle}$ now, and we know with the parameters of peaks of P_{3s} that the electrons initially localized in the fourth dot would be trapped completely in the third, fourth and fifth dots. In this figure, the peaks of P_{3s} include the peaks of $P_{|4,4\rangle,|4,4\rangle}$, which is very natural because electrons localized in fourth dot are also trapped in the middle three dots. However, when the parameter deviates from the localization peaks of $P_{|4,4\rangle,|4,4\rangle}$ slightly, the localization in the fourth dot is destroyed while the electrons are still trapped in the middle three dots, which actually means that the electrons oscillate in the middle three dots. If the field parameter further deviates from the localization peaks, then the oscillation region becomes larger, as shown in figure 1(b): the blue dashed peak of P_{5s} includes the peaks of P_{3s} . Under this condition, the electrons cannot reach the boundary dots (first and seventh dot) and the oscillation region can still be exactly controlled.

Figure 1(b) implies an effective way to control the electron position. The external ac driving field can be used as a key and we can use this key to control the gate of barrier. Using figure 1(b), we can easily open or close any barriers which we need to control, for example, the barrier between the third and fourth dots or the barrier between the second and third, and what we need to do is simply choose different ac field parameters in different peaks, which is very easy to be realized.

In figure 1(c), we present the curves of $P_{|4,4\rangle,|4,4\rangle}$ and P_{double} , where $P_{\text{double}} = \sum_{i=1}^7 P_{|4,4\rangle,|i,i\rangle}$, which describes the LAOP of two electrons moving together. In figure 1(c),

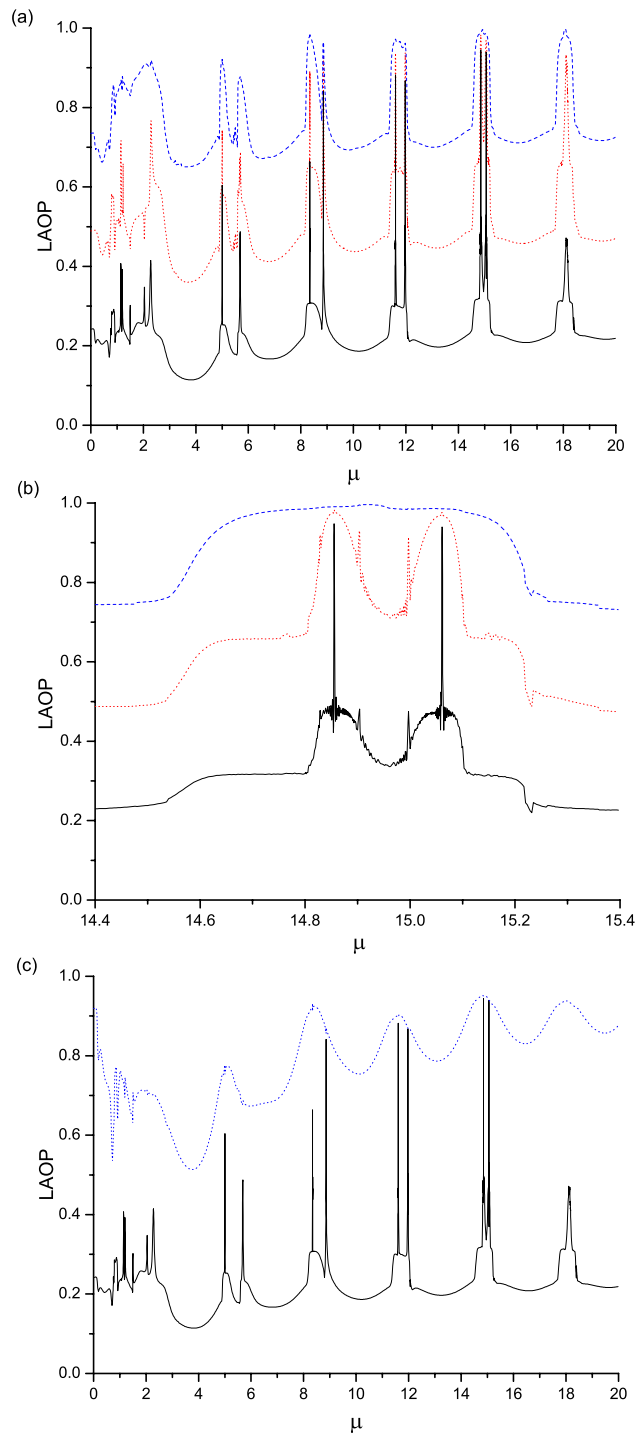


Figure 1. (a) The LAOP as a function of μ with $W/\omega = 0.25$: the black solid line describes the LAOP of $P_{[4,4],[4,4]}$; the middle (red) dotted line describes the LAOP of P_{3S} ; the top (blue) dashed line describes the LAOP of P_{5S} . (b) Amplification of one part of (a). (c) The LAOP of $P_{[4,4],[4,4]}$ and P_{double} . The dashed line corresponds to the P_{double} .

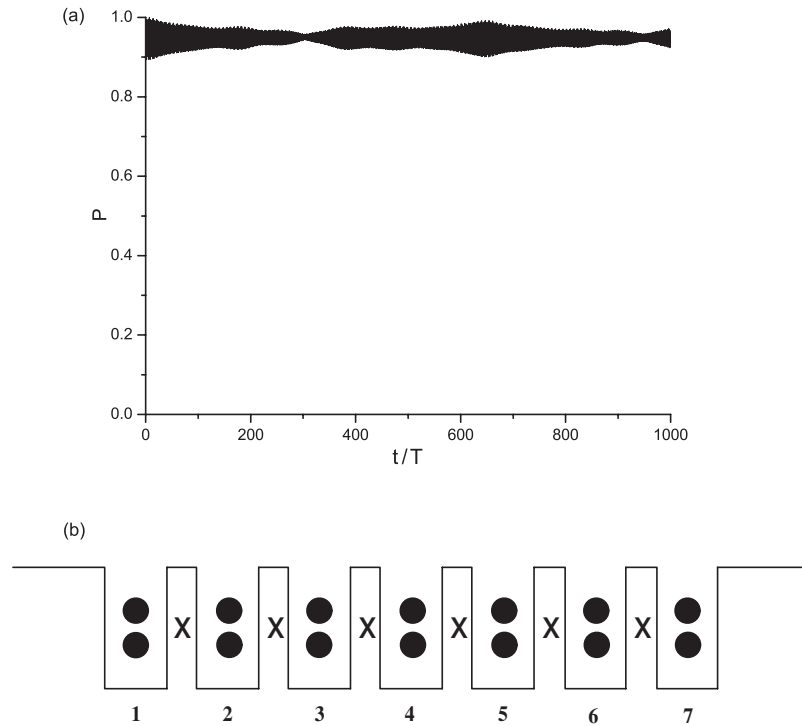


Figure 2. (a) The time evolution of the occupation probability $P(t)$ in the fourth dot with $\mu = 14.8553$. (b) The schematic representation of the dynamics.

the blue dashed line represents the P_{double} , and we can easily find that, in general, the nearer the parameter is to the localization peaks, the more the electrons move together. If the selected parameter significantly deviates from the localization peaks, on the other hand, the two electrons may be separated and move alone.

We examine the dynamical evolution of the occupation probability $P(t)$ through integrating equation (2) numerically. We first select a parameter in the localization peak $P_{|4,4\rangle,|4,4\rangle}$ in figure 1(b) with $\mu = 14.8553$. As shown in figure 2(a), the initial localized electrons always contain their initial state with the time evolution. We represent the dynamics of the system with $\mu = 14.8553$ schematically in figure 2(b). In this figure, a full circle means the electron is localized in that dot and a cross indicates the suppression of tunnelling through that barrier. Since the field parameter is selected in the localization peak of $P_{|4,4\rangle,|4,4\rangle}$, the barrier between the third and fourth dots is closed and the electrons cannot pass through it. Because the system is symmetric, the barrier between the fourth and fifth dots is closed too. Through further study, we find that, with initial double occupation states, the barriers among the first, second and third (fifth, sixth and seventh) dots are also closed in this condition and if localized in the first, second or third (fifth, sixth or seventh) dots initially, these two electrons will be completely localized forever.

We first open the barrier between the third and fourth (fourth and fifth) dots by choosing the parameter $\mu = 14.875$ in the peak region of P_{3s} . In figure 3(a), we present the occupation probability of electrons with states $|3, 3\rangle$, $|4, 4\rangle$ and $|5, 5\rangle$ (the initial state is $|4, 4\rangle$). Since the third dot and fifth dot are completely symmetric, the occupation probability evolutions of $|3, 3\rangle$ and $|5, 5\rangle$ are completely identical in this figure. In figure 3(a), we can see that if we investigate

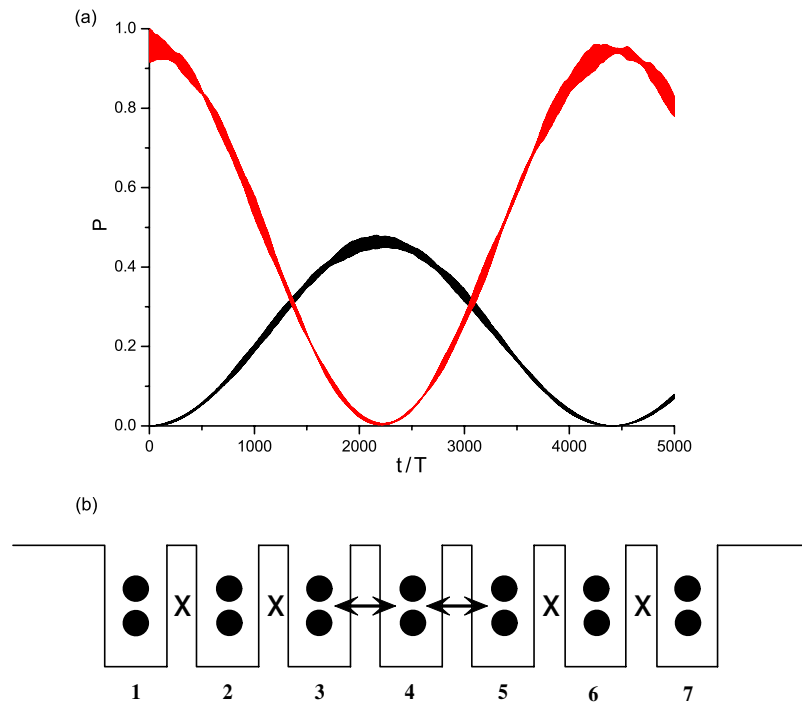


Figure 3. (a) The time evolution of the occupation probability $P(t)$ in $|3, 3\rangle$, $|4, 4\rangle$ and $|5, 5\rangle$ with $\mu = 14.875$. (b) The schematic representation of the dynamics.

the system with sufficiently long time, the electrons can oscillate between states $|4, 4\rangle$ and $|3, 3\rangle$ ($|5, 5\rangle$). This oscillation is dominated by the double occupation states, which can be explained by figure 1(c). It is clear that the barrier between the third and fourth dots (fourth and fifth dots) is open now, and the electrons can penetrate it with double occupation states. The barriers among the first, second and third dots (fifth, sixth and seventh dots), however, are still closed; this forbids the electrons to pass through them with initial double occupation states, and the electrons can only oscillate in the middle three dots. If the initial state is $|3, 3\rangle$ ($|5, 5\rangle$), since the barrier between the second and third dots (fifth and sixth dots) is closed to the double occupation state, the electrons still cannot reach the second and sixth dots and can only oscillate in the middle three dots. We present the dynamics under this condition in figure 3(b).

Let us now further open the barrier between the second and third dots (fifth and sixth dots). With $\mu = 14.7$, in figure 4(a) we can see that the electrons oscillate among the states of $|2, 2\rangle$, $|3, 3\rangle$ and $|4, 4\rangle$ (the $|5, 5\rangle$ and $|6, 6\rangle$ states are the same as $|2, 2\rangle$ and $|3, 3\rangle$). In this condition, the barrier between the second and third dots (fifth and sixth dots) is also opened to the initial double occupation state electrons. But the barrier between the first and second dots (sixth and seventh dots) is closed, and the electrons cannot reach these two boundary dots. Using any one among those above five double occupation states (from $|2, 2\rangle$ to $|6, 6\rangle$) as the initial state, we found that these two electrons always oscillate in these five states, which is shown in figure 4(b). If the initial state is $|1, 1\rangle$, since the electrons cannot penetrate the barrier between the first and second dots, they will be localized in the first dot completely. Moreover, if the selected parameter deviates further from the localization peaks, these two electrons will oscillate in the whole QD array, and in figure 1(a), we can see that this case is more common than cases with any kind of localization property.

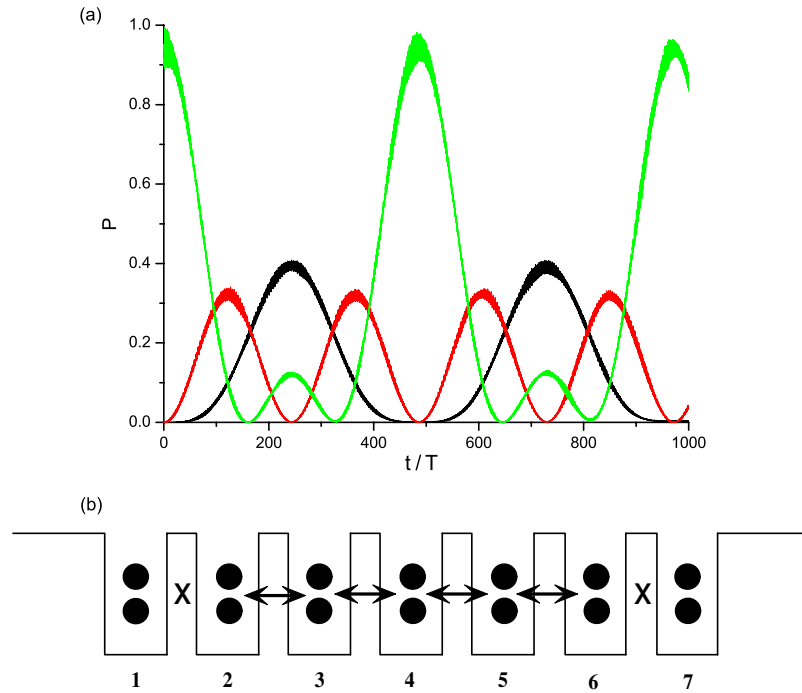


Figure 4. (a) The time evolution of the occupation probability $P(t)$ in $|2, 2\rangle$, $|3, 3\rangle$, $|4, 4\rangle$, $|5, 5\rangle$ and $|6, 6\rangle$ with $\mu = 14.7$. (b) The schematic representation of the dynamics.

We have known that with any values of the peaks of P_{3s} (the case of P_{5s} is similar), the electrons can oscillate in the determined region. However, the oscillation frequency is different with different parameters, it is determined by the deviation from the selected parameter from the position of the nearest localization peaks ($P_{|4,4\rangle,|4,4\rangle}$ here). The closer the selected parameters are to the localization peak, the lower the oscillation frequency becomes. The reason is that when the selected parameter approaches the localization peak, the velocity of the delocalization process significantly decreases, which decreases the oscillation frequency. We can clearly see this through comparing the figure 3(a) with 4(a). The time that the electrons completely leave the fourth dot (the occupation probability of electrons in the fourth dot approaches zero) is nearly 2200 driving periodicities. In contrast, in figure 4(a), to completely leave the fourth dot, the electrons only need 160 driving periodicities, which is much less than that in figure 3(a). The reason is that in this case, the deviation from its field parameter to the nearest localization peak $\Delta\mu \approx 0.155$, which is much larger than that in figure 3(a). Thus, to get a good oscillation effect, we should make this deviation from the selected parameter to nearest localization peak as large as possible. However, with the increase of this deviation, the oscillation region increases quickly, so this deviation cannot be too large and it must be balanced between the oscillation frequency and oscillation region.

Through the above discussion, we can see that the penetrability of the barrier can be arbitrarily and precisely controlled by adjusting the ac field magnitude among different peaks of the LAOP. Therefore, we can discretionarily open or close the gate of a barrier and control the electrons' position in principle. This control effect may be explained by the deviation of the selected field parameter to the localization peaks: since the selected parameter deviates from the localization peaks, the dynamical localization is destroyed; but because the deviation is slight, the electrons cannot move in the whole QD array immediately and still contain some

kind of localization property, which is represented as the manipulation of tunnelling. If the deviation of the selected parameter from the localization peaks is large enough, then all barriers should be opened and the electrons can oscillate in the whole QD array.

4. Manipulation of tunnelling with initial single occupation state

In this section, we study the dynamics of a system with initial state $|3, 5\rangle$. As in the previous section, we first present the LAOP of the system as a function of μ , as shown in figure 5(a). In this figure, the black solid line describes the LAOP of $P_{|3,5\rangle,|3,5\rangle}$. The red dotted line describes the P_{3s} and the blue dashed line corresponds to the P_{5s} , where the definitions of P_{3s} and P_{5s} are nearly identical to those in the previous section and the only difference is that the initial state here is $|3, 5\rangle$ whereas it was $|4, 4\rangle$ there. In this figure, we can see sharp peaks for all of these three curves, and we then magnify one part of this figure. In figure 5(b), we can see there is a high peak of $P_{|3,5\rangle,|3,5\rangle}$, which means that these two electrons can maintain their initial state with the parameter of this peak. The peak of P_{3s} is completely superimposed with $P_{|3,5\rangle,|3,5\rangle}$, and therefore it is impossible to restrict these two electrons in the middle three dots when the localization in their initial state $|3, 5\rangle$ is destroyed under this condition. There are two peaks of P_{5s} in figure 5(b) and we know with the parameter of the left peak that these two electrons will oscillate in the middle five dots.

In figure 5(c), we present the LAOP of $P_{|3,5\rangle,|3,5\rangle}$ and P_{single} , where $P_{\text{single}} = 1 - \sum_{i=1}^7 P_{|3,5\rangle,|i,i\rangle}$, which means the probability of two electrons moving separately. In this figure, we can see that these two initial discrete electrons always move separately. The double occupation states are nearly impossible to appear with such an initial condition. Comparing it with figure 1(c), we can see that it is more difficult to make two initial discrete electrons congregate than to separate two initial congregate electrons, which would result from the effect of the Coulomb interaction between electrons. In this figure, there is also a small fluctuation in the P_{single} , and when the localization peaks of $P_{|3,5\rangle,|3,5\rangle}$ appear, the P_{single} is relatively large, which is similar to figure 1(c).

Now we examine the above results through integrating numerically. We first select a localization point in figure 5(b) with $\mu = 11.79153$ and present the time evolution of state $|3, 5\rangle$ in figure 6(a). In this figure, one can see that these two electrons are completely localized in the third and fifth dots. Through further study, we find that if the initial state is $|1, 3\rangle$ or $|5, 7\rangle$, these two electrons can also maintain their initial state forever under this condition, and with other initial single occupation states, the initial states cannot be maintained, which implies that the case of initial single occupation states is much more complicated than that of initial double occupation states.

Since these two electrons cannot oscillate in the middle three dots with initial state $|3, 5\rangle$ under this condition, we select a parameter in the left peak of P_{5s} to trap these two electrons in the middle five dots. With $\mu = 11.78$, we can see in figure 6(b) that these two electrons oscillate among states $|2, 4\rangle, |2, 5\rangle, |2, 6\rangle, |3, 5\rangle, |3, 6\rangle$ and $|4, 6\rangle$ (the $|3, 6\rangle$ and $|4, 6\rangle$ are the same as $|2, 4\rangle$ and $|2, 5\rangle$). This oscillation is completely restricted in these six states and other states hardly appear in the time evolution. If we choose any other state among these six states to be the initial state, the results will be similar and the oscillation will still be restricted in these six states. This can explain why the peak of P_{3s} is completely superimposed with the peak $P_{|3,5\rangle,|3,5\rangle}$ in figure 5(b): with initial state $|3, 5\rangle$, the state of $|3, 5\rangle$ is the only possible state in the middle three dots near the peaks of P_{5s} , and if the localization in $|3, 5\rangle$ is destroyed, these electrons cannot be trapped in the middle three dots.

We have stated that with $\mu = 11.78$ and initial state $|3, 5\rangle$, the two electrons will oscillate in the middle five dots. However, if the initial single occupation state is not a member of those

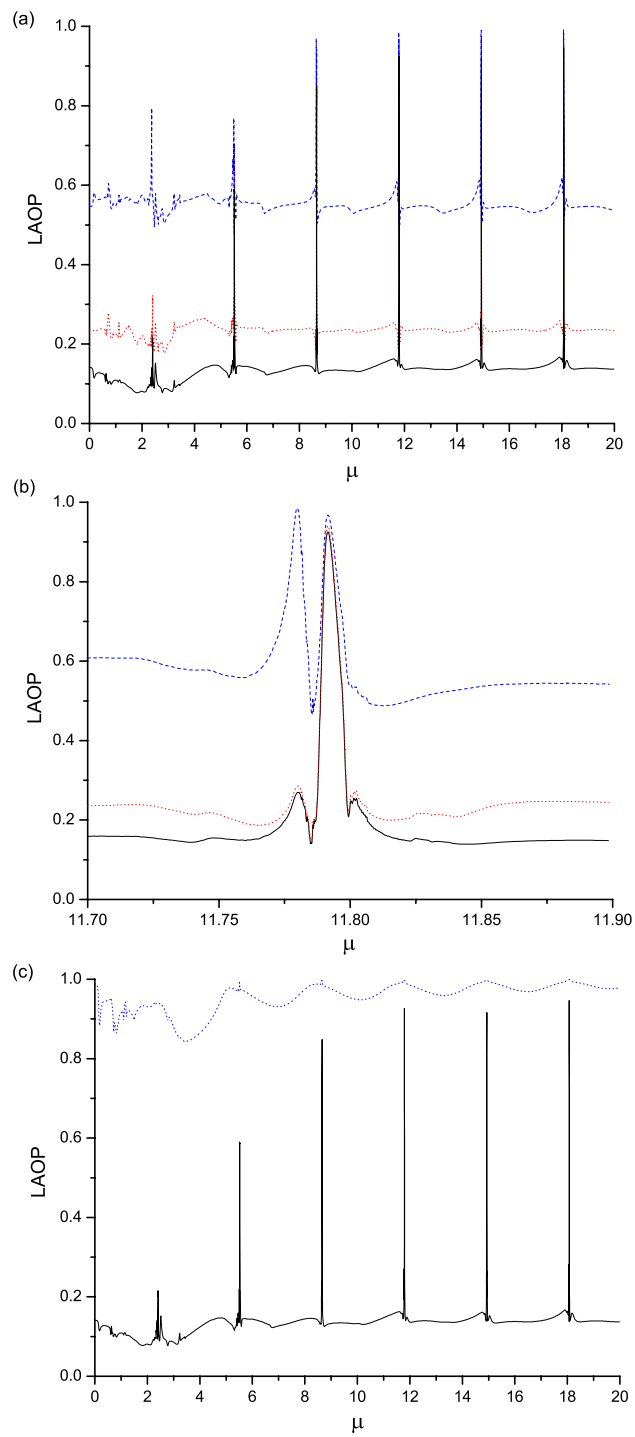


Figure 5. (a) The LAOP as a function of μ with $W/\omega = 0.25$: the black solid line describes the LAOP of $P_{[3,5],[3,5]}$; the middle (red) dotted line describes the LAOP of P_{3S} ; the top (blue) dashed line describes the LAOP of P_{5S} . (b) Amplification of one part of (a). (c) The LAOP of $P_{[3,5],[3,5]}$ and P_{single} . The dashed line corresponds to the P_{single} .

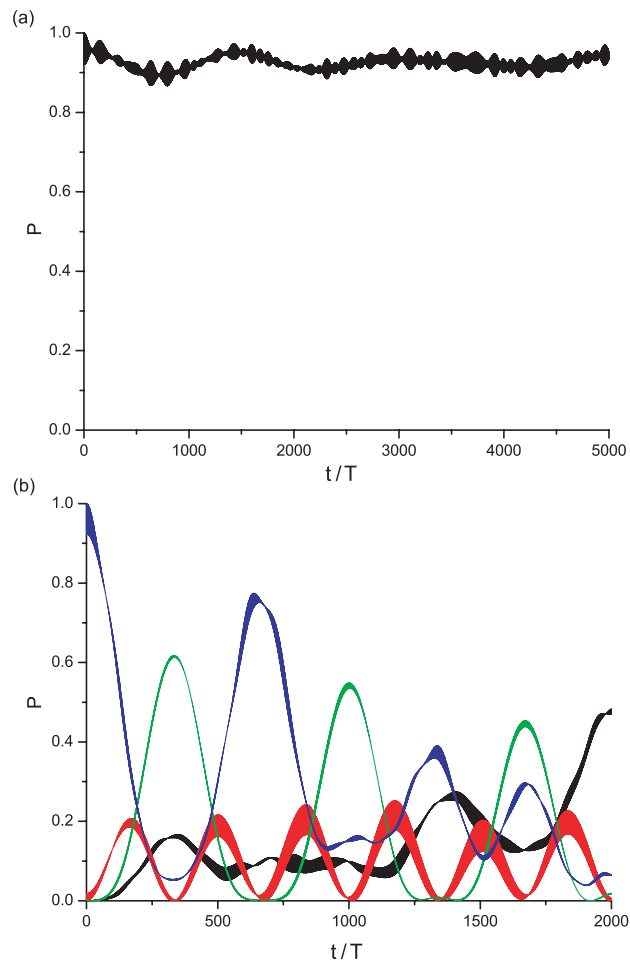


Figure 6. (a) The time evolution of the occupation probability $P(t)$ in $|3, 5\rangle$ with $\mu = 11.79153$. (b) The time evolution of the occupation probability $P(t)$ in $|2, 4\rangle$, $|2, 5\rangle$, $|2, 6\rangle$, $|3, 5\rangle$, $|3, 6\rangle$ and $|4, 6\rangle$ with $\mu = 11.78$.

above six states, the results are different. Through study we find that with $\mu = 11.78$ and initial state $|2, 3\rangle$, these two electrons will oscillate among states $|1, 2\rangle$, $|2, 3\rangle$, $|3, 4\rangle$, $|4, 5\rangle$, $|5, 6\rangle$, $|6, 7\rangle$ and be completely trapped in these six states. These two kinds of states are very different electron configurations and the difference in electron configuration leads to the difference of barrier penetrability. In addition, if the initial state is $|1, 7\rangle$, these electrons will be localized under this condition. Moreover, if the selected parameter further deviates from the localization peaks, with initial state $|3, 5\rangle$, these two electrons will oscillate in the whole QD array, which is much more popular than being trapped in any group of dots, as shown in figure 5(a).

Through the above discussion, we know that it is still possible to manipulate the tunnelling with initial single occupation states. The double occupation state and single occupation state are basically insulated in the process of manipulation of tunnelling, as shown in figures 1(c) and 5(c), so they can be discussed separately. The case of initial single occupation state is more complicated in that there also have different electron configurations in the single occupation state itself.

5. The physical explanation of manipulation of tunnelling

Since the Floquet approach is the universal method in the field of CDT, we here introduce the Floquet spectrum to further study the physical process discussed above. With the same parameters as figure 1(a), we present the Floquet spectrum of the system in figure 7(a). In this figure, we can see that, in the weak field region, the Floquet spectrum is very complicated, but with the increase of ac field magnitude, the Floquet spectrum divides into two minibands. The upper miniband contains 7 quasi-energy levels, and the other 21 quasi-energy levels form the lower miniband. There are apparent collapse zones for both of these two minibands and many works [24–26] have pointed out that, at the collapse zone of quasi-energy levels, the system represents the property of localization.

Now we study the relations between the localization peaks of the LAOP and the Floquet spectrum. In figure 7(b), we enlarge one collapse point of figure 7(a) and superimpose it with one part of figure 1(b). Here we subtract 0.64 from the value of LAOP to make the peaks of LAOP and the quasi-energy levels comparable. Since the value region of the vertical axis in figure 7(b) is as small as $\Delta\text{LAOP} \in [0.931, 0.939]$, the curves in figure 1(b) become straight lines in this figure and we know that the black solid lines mean the localization peaks of $P_{|4,4\rangle,|4,4\rangle}$. Similarly, the region between two neighbouring red dotted line corresponds to the peak of P_{3s} and that between two neighbouring blue dashed lines represents the peak of P_{5s} . For the reason that $\Delta\varepsilon \in [0.291, 0.299]$ in this figure, it is clear that these seven quasi-energy levels belong to the upper miniband shown in figure 7(a). In figure 7(b), we can see both of these two localization peaks accurately correspond to the crossing points of quasi-energy levels, which can explain why the dynamical localization happens under this condition with the initial double occupation state. In this figure, we can also see that when the selected parameter slightly deviates from those two crossing points, these two electrons oscillate in the middle three dots and the five dot oscillation region nearly includes the whole collapse region of quasi-energy levels.

Concerning figure 7(b), there are another two points that should be mentioned. First, although those two localization peaks exactly correspond to two crossing points, there are still other crossing points in this figure and we can see that those crossing points do not exhibit any special dynamics property. Second, in figure 1(c), we can clearly see that although the localization always happens in the upper miniband collapse zones, the localization effect is very different. Therefore, if we only study the CDT with the help of the Floquet spectrum, it is difficult to get a clear comprehension of the dynamics of system, in particular in such a complex system. The LAOP method, however, can give an intuitionistic and quantitative description of system, and therefore can be widely used.

We then study the relations between the localization peaks of the LAOP and the Floquet spectrum with an initial single occupation state. In figure 7(c), we enlarge one collapse point of figure 7(a) and superimpose it with one part of figure 5(b), and here we subtract 0.9 from the value of LAOP. For the reason that $\Delta\varepsilon \in [-0.006, 0.01]$ in this figure, it is clear that these 21 quasi-energy levels belong to the lower miniband shown in figure 7(a). In this figure, we can see that the region of the level collapse is in fact a region with several crossings and anticrossings. One can clearly see that the zone between the two black solid lines, which means the localization peak of $P_{|3,5\rangle,|3,5\rangle}$, corresponds to the exact crossing points of quasi-energy levels. The three dot oscillation region nearly superimposes with the localization peak and the five dot oscillation region divides into two parts. The right peak includes the localization peak of $P_{|3,5\rangle,|3,5\rangle}$ and the left peak corresponds to the anticrossing points of quasi-energy levels.

Through the above discussion, we can find that these two minibands of quasi-energy describe different physical process. The upper miniband corresponds to the physical process

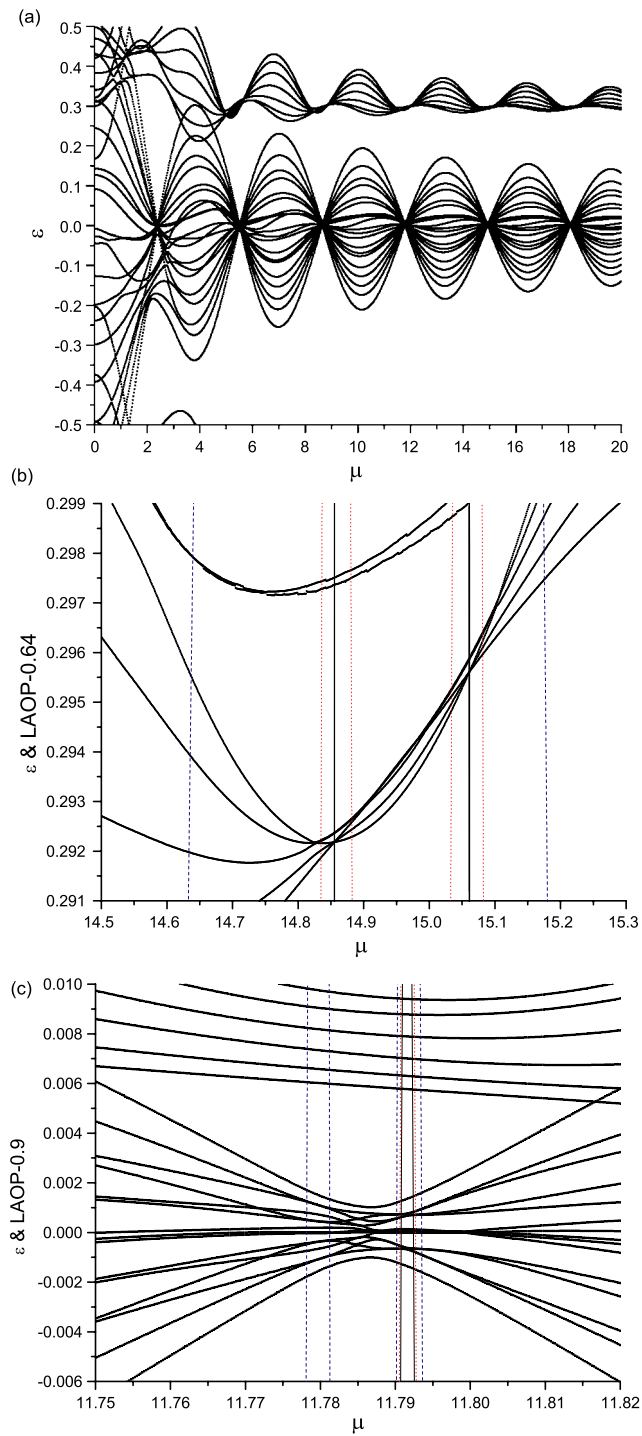


Figure 7. (a) The Floquet spectrum of the system. (b) The Floquet spectrum and LAOP = 0.64 with initial state $|4, 4\rangle$. (c) The Floquet spectrum and LAOP = 0.9 with initial state $|3, 5\rangle$.

of a double occupation state and the number of quasi-energy levels belonging to it is the same as the number of QDs contained in the array, which also equates with the number of double occupation states. The lower miniband corresponds to the physical process of a single occupation state, which includes all other quasi-energy levels. Since these two kinds of states belong to different quasi-energy minibands, it is natural to divide them into two groups, and therefore we can study the dynamics of them separately, just as we have done above. In figure 1(c) and 5(c), there is an apparent phenomenon that the transition between these two kinds of states happens more easily in the weak field region, and now we can explain it through figure 7(a). In figure 7(a), we can see that, in the weak field region, these two quasi-energy minibands overlap and cannot be clearly separated, which leads to the transition between these two kinds of states. With the increase of ac field magnitude, the difference between these two minibands is more and more distinct, and therefore the transition between these two kinds of states is more and more difficult.

In figure 7(a), there are apparent periodic collapse points in the lower miniband. Through studying the values of those collapse points, we find that the lower miniband collapses when $\mu \simeq 2.4, 5.52, 8.65, 11.79, \dots$, which clearly accord with the roots of the zeroth Bessel function. It is well known that when the ratio of the strength of the driving field to the driving frequency is the root of the zeroth Bessel function, the quasi-energy band collapses with the one-electron model [21, 27]. Therefore, it is very interesting that the positions of lower miniband collapse points in figure 7(a) are completely identical with those of the one-electron model. This intriguing phenomenon results from the Hubbard-type Hamiltonian (equation (9)) we studied in this paper. In equation (9), we only consider the Coulomb interaction when two electrons locate in one dot; however, in the last section, we have found that the two initial separate electrons always move separately and it is difficult to make them congregate, as shown in figure 5(c). Therefore, with an initial single occupation state, the Coulomb interaction has only a little effect on the dynamics of system, which results in the similarity between the case of the initial single occupation state and the one-electron model. Further, if we compare figure 7(c) with the results of Villas-Boas [21], we can find that the quasi-energy spectrum structures of those two kinds of system are also alike.

At the end of this paper we discuss the experimental conditions to investigate the manipulation effect. We know the coupling parameter W can be set by regulating the height of the interdot tunnelling barriers and U by adjusting the size of the QD. A recent experiment [28] gave estimates of $U \simeq 3.7$ meV and $W \simeq 0.5$ meV in a double QD system. Given that the QD separation was about 200 nm, the required driving field to see the manipulation effects we reported should be of the order of 400 GHz, with field strengths of up to 1.7 kV cm⁻¹.

6. Conclusions

In summary, using the LAOP method, we present an approach to control coherently the electronic position in a QD array with the two-electron model. The electrons will localize in the QD array with appropriate parameters and will oscillate in the array when the field parameter deviates from the values of the localization peaks. Through tuning the external ac driving field, we can easily open the barriers one by one and enlarge the oscillation regime of the electrons, which provides a method to exactly control the penetrability of the barrier. The oscillation frequency is determined by the deviation from the selected field parameter to the parameter of the nearest localization peak. The nearer the selected parameter is to the localization peak, the lower the oscillation frequency becomes. The Floquet spectrum of the system can be divided into two minibands. The upper miniband corresponds to the physical process of a double occupation state and the lower miniband describes that of a single occupation state. Since

these two kinds of states belong to different quasi-energy minibands, they are insulated in the manipulative process, in particular in the medium and strong field region, and therefore can be discussed separately. The results of these two kinds of initial states are basically consistent. The case of an initial single occupation state is more complicated because it can be further divided into different electron configurations, and with different electron configuration, the penetrability of the barrier is dissimilar. Since these two initial separate electrons can hardly be congregated, the Coulomb interaction has little effect on them and the behaviour of them is similar to that from the one-electron model. We believe that this method makes it possible to manipulate the position of electrons and can be useful in quantum computation.

Acknowledgments

This work is supported in part by the National Natural Science Foundations of China under Grant No. 10274007, and a grant from the China Academy of Engineering and Physics.

References

- [1] Loss D and DiVincenzo D P 1998 *Phys. Rev. A* **57** 120
- [2] Lloyd S 1993 *Science* **261** 1589
- [3] DiVincenzo D P 1995 *Science* **269** 255
- [4] Grossmann F, Dittrich T, Jung P and Hänggi P 1991 *Phys. Rev. Lett.* **67** 516
- [5] Grossmann F and Hänggi P 1992 *Europhys. Lett.* **18** 571
- [6] Zhao X-G 1994 *Phys. Lett. A* **193** 5
- [7] Hao W and Zhao X-G 1996 *Phys. Lett. A* **217** 225
- [8] Creffield C E and Platero G 2002 *Phys. Rev. B* **65** 113304
- [9] Zhang P and Zhao X-G 2000 *Phys. Lett. A* **271** 419
- [10] Paspalakis E and Terzis A F 2004 *J. Appl. Phys.* **95** 1603
- [11] Creffield C E and Platero G 2002 *Phys. Rev. B* **66** 235303
- [12] Jiang Z, Suqing D and Zhao X-G 2004 *Phys. Lett. A* **333** 132
- [13] Creffield C E and Platero G 2004 *Phys. Rev. B* **69** 165312
- [14] Noba K-I 2003 *Phys. Rev. B* **67** 153102
- [15] Zhang C 2002 *Phys. Rev. B* **66** 081105(R)
- [16] Zhang C and Cao J C 2004 *Phys. Rev. B* **70** 193311
- [17] Platero G and Aguado R 2004 *Phys. Rep.* **395** 1
- [18] Kohler S, Lehmann J and Hänggi P 2005 *Phys. Rep.* **406** 379
- [19] Holthaus M 1992 *Phys. Rev. Lett.* **69** 351
- [20] Zhao X-G 1997 *Phys. Lett. A* **230** 229
- [21] Villas-Boas J M, Ulloa S E and Studart N 2004 *Phys. Rev. B* **70** 041302
- [22] Jiang Z, Suqing D and Zhao X-G 2004 *Phys. Lett. A* **330** 260
- [23] Grifoni M and Hanggi P 1998 *Phys. Rep.* **304** 229
- [24] Creffield C E 2003 *Phys. Rev. B* **67** 165301
- [25] Suqing D, Wang Z-G and Zhao X-G 2003 *Chin. Phys.* **12** 0899
- [26] Zhang A-Z, Zhang P, Suqing D, Zhao X-G and Liang J-Q 2001 *Phys. Rev. B* **63** 045319
- [27] Suqing D, Wang Z-G, Wu B-Y and Zhao X-G 2003 *Phys. Lett. A* **320** 63
- [28] Elzerman J M, Hanson R, Greidanus J S, Willems van Beveren L H, De Franceschi S, Vandersypen L M K, Tarucha S and Kouwenhoven L P 2003 *Phys. Rev. B* **67** 161308